(1 equiv CH_2Cl_2 of crystallization also observed); $[\alpha]_D^{25.4} = -1.03$ ($c = 1.01$ in CH_2Cl_2); elemental analysis calcd for $C_{46}H_{36}O_2P_2Pt \cdot CH_2Cl_2$: C 58.6, H 4.0; found: C 58.2, H 4.0.

[7] Crystal data for **2a**: $a = 12.5114(7)$, $b = 17.0838(10)$, $c = 18.3107(10)$ Å, $V = 3913.8(4)$ Å^3, orthorhombic, space group $P2_12_12_1$, crystal dimensions $0.05 \times 0.05 \times 0.40$ mm, $\rho_{calc} = 1.634$ Mg m^{-3}, $Z = 4$, $2\theta_{max} = 50.0°$. X-ray data were collected at -100 °C on a Siemens SMART diffractometer with CCD detection and $Mo_{K\alpha}$ radiation ($\lambda = 0.71073$ Å) in the ω scan mode. Of 20439 reflections collected, 6903 were unique and 5370 were included in subsequent calculations. Correction of the intensity data by using the SADABS program gave a range of relative corrections of 0.733–1.76 and an absorption correction of $\mu = 3.83$ mm^{-1}. The structure was solved by direct methods. In the final least-squares refinement cycle, non-hydrogen atoms were refined anisotropically, and hydrogen atoms were included with a riding model. The quantity minimized was $Sw|D|F|^2$. The model converged at $R = 0.042$, $wR = 0.042$, and GOF = 1.15 for 5335 reflections with $I_{net} > 2.5\sigma(I_{net})$ and 487 parameters. Calculations were performed with the program NRCVAX. Crystallographic data (excluding structure factors) for the structures reported in this paper have been deposited with the Cambridge Crystallographic Data Centre as supplementary publication no. CCDC-101092. Copies of the data can be obtained free of charge on application to CCDC, 12 Union Road, Cambridge CB2 1EZ, UK (fax: (+44) 1223-336-033; e-mail: deposit@ccdc.cam.ac.uk).

[8] a) S. Masamune, W. Choy, J. S. Petersen, L. R. Sita, *Angew. Chem.* **1985**, *97*, 1–78. *Angew. Chem. Int. Ed. Engl.* **1985**, *24*, 1–76; b) T. Ohkuma, H. Doucet, T. Pham, K. Mikami, T. Korenaga, M. Terada, R. Noyori, *J. Am. Chem. Soc.* **1998**, *120*, 1086–1087; c) K. Mikami, S. Matsukawa, T. Volk, M. Terada, *Angew. Chem.* **1997**, *109*, 2936–2939; *Angew. Chem. Int. Ed. Engl.* **1997**, *36*, 2768–2770; d) K. Burgess, M. J. Ohlmeyer, K. H. Whitmire, *Organometallics* **1992**, *11*, 3588–3600.

[9] (*S*)-**2b**: ^{31}P NMR (121.5 MHz, CD_2Cl_2): $\delta = 30.3$, $^1J_{P,Pt} = 3547$ Hz; ^{1}H NMR (300 MHz, CD_2Cl_2): $\delta = 7.86$ (m, 8H), 7.66 (m, 4H), 7.51 (m, 12H), 7.05 (dd, $J = 7.7$, 6.9 Hz, 2H), 6.95 (dd, $J = 8.3$, 6.8 Hz, 2H), 6.79 (d, $J = 8.5$ Hz, 2H), 6.59 (d, $J = 8.8$ Hz, 2H), 2.28 (m, 2H, CH), 1.05 (m, 2H, CH_3) (0.5 equiv Et_2O of crystallization also observed); $[\alpha]_D^{24.7} = -151.6$ ($c = 1.02$ in CH_2Cl_2); elemental analysis calcd for $C_{48}H_{40}O_2P_2Pt \cdot 0.5\,C_4H_{10}O$: C 63.7, H 4.8; found: C 63.9, H 4.9. (*R*)-**2b**: ^{31}P NMR (121.5 MHz, $CDCl_3$): $\delta = 31.8$, $^1J_{P,Pt} = 3562$ Hz; ^{1}H NMR (300 MHz, CD_2Cl_2): $\delta = 7.92$ (m, 4H), 7.83 (m, 4H), 7.74 (d, $J = 6.1$ Hz), 7.66 (m, 6H), 7.53 (m, 2H), 7.46 (m, 4H), 7.35 (d, $J = 8.8$ Hz, 2H), 7.03 (t, 2H), 6.90 (t, $J = 7.0$ Hz, 2H), 6.71 (d, $J = 8.6$ Hz, 2H), 6.00 (d, $J = 8.8$ Hz, 2H), 2.22 (m, 2H, CH), 1.04 (m, 6H, CH_3) (H_2O and Et_2O of crystallization also observed); $[\alpha]_D^{24.0} = +110.6$ ($c = 1.02$ in CH_2Cl_2); elemental analysis calcd for $C_{48}H_{40}O_2P_2Pt \cdot H_2O \cdot 0.375\,C_4H_{10}O$: C 62.5, H 4.85; found: C 61.9, H 4.55.

[10] The crystal structure analysis of (*s*)-**2b** was carried out as described in ref. [7]. Crystal data: $a = 13.4508(6)$, $b = 17.5011(8)$, $c = 19.0202(9)$ Å, $V = 4477.4(4)$ Å^3, orthorhombic, space group $P22_12_1$, crystal dimensions $0.20 \times 0.20 \times 0.08$ mm, $\rho_{calcd} = 1.399$ Mg m^{-3}, $Z = 4$, $2\theta_{max} = 55.0°$. Of 36189 reflections collected, 10236 were unique and 9052 were included in the refinement. Correction of the intensity data by using the program SADABS gave a range of relative corrections of 0.816–1.136 and an absorption correction $\mu = 3.23$ mm^{-1}. In the final least-squares cycle, the model converged at $R = 0.050$, $wR = 0.059$, and GOF = 2.47 for 9031 reflections with $I_{net} > 2.5\sigma(I_{net})$ and 538 parameters.

[11] a) R. Argazzi, P. Bergamini, V. Gee, J. K. Hogg, A. Martín, A. G. Orpen, P. G. Pringle, *Organometallics* **1996**, *15*, 5591–5597; b) D. H. Farrar, N. C. Payne, *J. Am. Chem. Soc.* **1985**, *107*, 2054–2058; c) J. M. Brown, P. L. Evans, P. J. Maddox, K. H. Sutton, *J. Organomet. Chem.* **1989**, *359*, 115–125; d) C. G. Young, S. J. Rettig, B. R. James, *Can. J. Chem.* **1986**, *64*, 51–56; e) A. S. C. Chan, J. J. Pluth, J. Halpern, *J. Am. Chem. Soc.* **1980**, *102*, 5952–5954.

[12] The crystal structure analysis of (*R*)-**2b** was carried out as described in ref. [7]. Crystal data: $a = b = 46.8015(23)$, $c = 16.1220(8)$ Å, $V = 35313(3)$ Å^3, tetragonal, space group $P4_3$, crystal dimensions $0.20 \times 0.20 \times 0.15$ mm, $\rho_{calcd} = 1.429$ Mg m^{-3}, $Z = 4$, $2\theta_{max} = 50.0°$. Of 319032 reflections collected, 62211 were unique and 45551 were included in the refinement. Correction of the intensity data by using the program SADABS gave a range of relative corrections of 0.700–1.223 with $\mu = 3.28$ mm^{-1}. In the final least-squares cycle, the model converged at $R = 0.065$, $wR = 0.060$, and GOF = 1.91 for 44970 reflections with $I_{net} > 3.0\sigma(I_{net})$ and 4023 parameters. Because of the unusual size of this structure, care was taken to ensure that the cell and symmetry were correct. The program MISSYM was used both on the completed structure and on the Pt positions alone. No additional crystallographic or noncrystallographic symmetry elements or translations were detected.

[13] J. S. Giovannetti, C. M. Kelly, C. R. Landis, *J. Am. Chem. Soc.* **1993**, *115*, 4040–4057.

[14] a) J. M. Clemente, C. Y. Wong, P. Bhattacharyya, A. M. Z. Slawin, D. J. Williams, J. D. Woollins, *Polyhedron* **1994**, *13*, 261–266; b) K. Osakada, Y. Kim, A. Yamamoto, *J. Organomet. Chem.* **1990**, *382*, 303–317; c) A. L. Seligson, R. L. Cowan, W. C. Trogler, *Inorg. Chem.* **1991**, *30*, 3371–3381; d) R. L. Cowan, W. C. Trogler, *J. Am. Chem. Soc.* **1989**, *111*, 4750–4761.

[15] The magnitude of the variations in the torsional angles observed here is also similar to that of dppe fragments in multiple-molecule crystal structures: A. Martín, A. G. Orpen, *J. Am. Chem. Soc.* **1996**, *118*, 1464–1470.

[16] See Table 1. For **2a**, the torsional angles at C1 and C3 indicate pseudoequatorial, and those at C2 and C4 pseudoaxial phenyl groups. For (*S*)-**2b** and (*R*)-**2b**, the torsional angles at C1 and C3 indicate pseudoaxial, and those at C2 and C4 pseudoequatorial phenyl groups. Note that the lack of C_2 symmetry in these molecules makes each of the four torsional angles unique. All molecules are viewed with positive ξ so that intermolecular comparisons between phenyl groups in the same quadrant are possible.

[17] For comparison, k_{obs} for **2a** is $2.1(1) \times 10^{-3}$ s^{-1}.

[18] a) D. Cai, D. L. Hughes, T. R. Verhoeven, P. J. Reider, *Tetrahedron Lett.* **1995**, *36*, 7991–7994; b) D. A. Slack, M. C. Baird, *Inorg. Chim. Acta* **1977**, *24*, 277–280; c) J. X. McDermott, J. F. White, G. M. Whitesides, *J. Am. Chem. Soc.* **1976**, *98*, 6521–6527; d) M. A. Andrews, G. L. Gould, W. T. Klooster, K. S. Koenig, E. J. Voss, *Inorg. Chem.* **1996**, *35*, 5478–5483.

The Hexanitridodimanganate(IV) $Li_6Ca_2[Mn_2N_6]$: Preparation, Crystal Structure, and Chemical Bonding**

Oliver Hochrein, Yuri Grin, and Rüdiger Kniep*

While the ternary nitrides $Li_7[V^VN_4]$[1, 2] and $Li_6[Cr^{VI}N_4]$[3] contain the 3d metals in their highest oxidation states, only the oxidation state +5 is attained by manganese in $Li_7[Mn^VN_4]$[1]. In the ternary systems Ca/(V,Cr,Mn)/N, only intermediate transition metal(III) compounds occur: $Ca_3[V^{III}N_3]$[4], $Ca_3[Cr^{III}N_3]$[5], $Ca_3[Mn^{III}N_3]$,[6] and $(Ca_3N)_2[Mn^{III}N_3]$[7]. In the quaternary system Li/Ca/Mn/N, we have now obtained $Li_6Ca_2[Mn_2N_6]$, a hexanitridodimanganate(IV). This is the first nitridometalate of a transition metal with an unbridged

[*] Prof. Dr. R. Kniep, Dipl.-Ing. O. Hochrein
Eduard-Zintl-Institut der Technischen Universität
Hochschulstrasse 10, D-64289 Darmstadt (Germany)
Fax: (+49) 6151-166029
Dr. Yu. Grin
Max-Planck-Institut für Festkörperforschung
Heisenbergstrasse 1, D-70569 Stuttgart (Germany)

[**] This work was supported by the Deutsche Forschungsgemeinschaft (Schwerpunktprogramm "Nitridobrücken) and by the Fonds der Chemischen Industrie.

  1433-7851/98/3711-1582 $ 17.50+.50/0

metal–metal bond within a complex anion.[8] It is also the first example of a Mn–Mn bond between manganese centers in the high oxidation state +4. The currently known compounds with unbridged Mn–Mn bonds contain Mn^0 and Mn^{-1} centers (e.g., $[Mn_2(CO)_{10}]$[9] and $(AsPh_4)[Mn_3(CO)_{14}]$[10]).

For the synthesis of $Li_6Ca_2[Mn_2N_6]$, a mixture of lithium, calcium, and manganese in a molar ratio of 6:1:1 was heated in a tantalum crucible to 900 °C over 2 h and subsequently treated with a stream of nitrogen at this temperature. After a reaction time of 60 h, the reaction mixture was cooled to room temperature over 6 h. $Li_6Ca_2[Mn_2N_6]$ was obtained as the main product together with some other phases that were not further investigated. The preparation of the quaternary compound also succeeds with a Li:Ca:Mn molar ratio of 3:1:1 under the same conditions, but the yield is considerably lower. $Li_6Ca_2[Mn_2N_6]$ forms platelike crystals with a silver-metallic luster and layer cleavage parallel to (001).

The crystal structure of $Li_6Ca_2[Mn_2N_6]$[11] is shown in Figure 1. The nitrogen atoms are arranged according to the motif of hexagonal close packing (stacking sequence AB); the

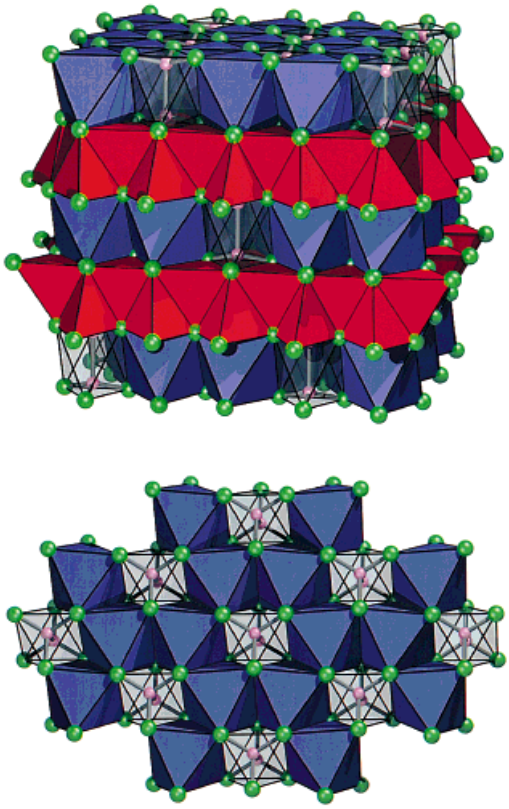

Figure 1. Section of the crystal structure of $Li_6Ca_2[Mn_2N_6]$ (top) and a section of the octahedral layer (bottom). Green spheres: nitrogen; blue octahedra: (N_6Ca); transparent octahedra: (N_6Mn_2); red tetrahedra: (N_4Li).

octahedral holes of every second double layer are occupied by an ordered arrangement of calcium ions and Mn_2 dumbbells in a ratio of 2:1. This $Ca_2[Mn_2N_6]^{6-}$ partial structure is closely related to that of the hexaselenodiphosphate(IV) $Mg_2[P_2Se_6]$ (space group $R3$, noncentrosymmetric variant[12]) and is an isotype of $CuAl[P_2Se_6]$ (space group $R\bar{3}$, statistical distribution of Cu and Al[13]). The negative charges of the anionic layer structure are compensated by Li^+ ions, which occupy all the tetrahedral holes between the octahedral layers filled by calcium and Mn_2 dumbbells.[14] The interatomic distances in the $Li_6Ca_2[Mn_2N_6]$ structure resemble those of known nitridomanganates,[15] with the exception of the Mn–Mn bond found here for the first time.

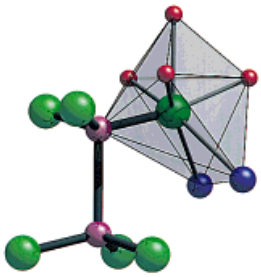

Figure 2. Complex anion $[Mn_2^{IV}N_6]^{10-}$ (staggered conformation) with cation coordination polyhedron around one nitrido position. Green spheres: nitrogen; violet spheres: manganese; red spheres: calcium; gray spheres: lithium. Selected interatomic distances [pm]: Li–N 200–221, Ca–N 252–264, Mn–N 178, Mn–Mn 236.[15]

A special feature of the $Li_6Ca_2[Mn_2N_6]$ structure is the hexanitridodimanganate(IV) anion (Figure 2) with a short Mn–Mn bond of 235.8(1) pm. Unbridged Mn–Mn bonds were formerly known only for Mn^0 and Mn^{-1} compounds, which exhibit Mn–Mn bond lengths of 289.5 pm ($Mn_2(CO)_{10}$[9]) and 288.3 and 290.6 pm ($(AsPh_4)[Mn_3(CO)_{14}]$[10]). The Mn–Mn distances in α-Mn lie between 224 and 291 pm.[16] The close relationship between the crystal chemistry of hexaselenodiphosphates(IV)[12, 13] and the hexanitridodimangante(IV) has already been mentioned; the complex anions show identical conformations (staggered arrangement), but strictly speaking are not isosteric ($[P_2Se_6]^{4-}$: 50 e^-; $[Mn_2N_6]^{10-}$: 54 e^-).

The electronic structure of $Li_6Ca_2[Mn_2N_6]$ was calculated by means of the TD-LMTO program (LDA approximation).[17] For the interpretation of the bonding situation, the electron localization function (ELF)[18] was evaluated. The ELF values are restricted by definition to the range between 0 and 1. High ELF values are characteristic of regions of high localization, such as in bonds or lone pairs. Specific details were obtained from the ELF by an analytical procedure that is also applied to the investigation of electron density.[19] By topological analysis, the total ELF field is partitioned into the basins of the core or bond attractors as well as the basins of the attractors of the lone pairs. The integration of the electron density in these regions yields the number of electrons belonging to them. For the bonding attractor, this procedure also provides information about bond order.[20–24]

The ELF for the crystal structure of $Li_6Ca_2[Mn_2N_6]$ is characterized by three symmetrically independent maxima in the unit cell (Figure 3). The highest ELF value (0.866) is exhibited by the lone pairs of the nitrido groups of the $[Mn_2N_6]$ units (Figure 3a). The deformation of these regions is caused by the repulsive interaction between the neighboring nitrido groups and by the polarizing influence of the coordinating cations. The next lower maximum, with an ELF value of 0.785 and a small basin, extends from the nitrido ligand towards the Mn center (Figure 3b). This attractor is located very close to the nitrogen atom and is thus representive of the pronounced polar character of the Mn–N bond. The third and most interesting type of local ELF maximum is found on the Mn–Mn connecting line (Figure 3c) and can

  1433-7851/98/3711-1583 $ 17.50+.50/0

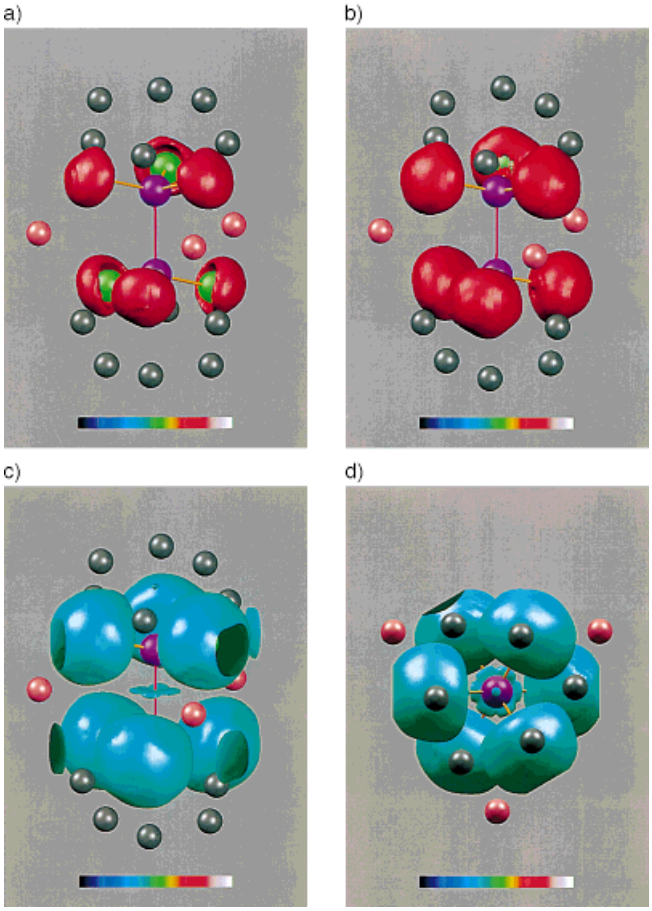

Figure 3. Isosurfaces of the electron localization function for $Li_6Ca_2[Mn_2N_6]$. Green spheres: nitrogen; violet spheres: manganese; red spheres: calcium, gray spheres: lithium. The connecting lines Mn – Mn and Mn – N are shown in red and orange, respectively. The colors of the ELF isosurfaces correspond to the ELF scale in the lower part of the figure. a) Attractors of the lone pairs at the nitrido positions (ELF = 0.866). b) Bonding attractors (ELF = 0.785) on the Mn – N connecting line (polar character of the Mn – N bonds). c) Bonding attractor Mn – Mn with the low ELF value of 0.392 (d character of the electron density[25]); two-electron, two-center bond (see text). View approximately perpendicular to the Mn – Mn bond. d) Bonding attractor Mn – Mn; view along the Mn – Mn bond.

assigned to a covalent interaction. The putative fourfold symmetry of this attractor evident in Figure 3c is in fact consistent with the threefold axis (space group $R\bar{3}$), as can be seen in Figure 3d with a view along the connecting line Mn – Mn. The relatively low ELF value in this maximum (0.392) is consistent with the predominant d character of the electron density in this region.[25] The integration of the electron density in the basin of this attractor gives 2.0 electrons; hence, the Mn – Mn bond should be regarded as a two-electron, two-center bond.

Till now investigations of the magnetic properties of $Li_6Ca_2[Mn_2N_6]$ have been affected by magnetically active impurities in the samples. Nevertheless, the measurements already indicate a weak temperature-dependent paramagnetism of the quaternary compound, presumably resulting from the electrons that do not participate in the bonds of the complex anion.

Received: January 8, 1997 [Z11339IE]
German version: *Angew. Chem.* **1998**, *110*, 1667 – 1670

Keywords: electronic structure · electron localization function · manganese · nitrides

[1] R. Juza, E. Anschütz, H. Puff, *Angew. Chem.* **1959**, *71*, 161.
[2] R. Juza, W. Gieren, J. Haug, *Z. Anorg. Allg. Chem.* **1960**, *300*, 61 – 71; C. Addison, M. G. Barker, J. Bentham, *J. Chem. Soc. Dalton Trans.* **1972**, 1035 – 1038.
[3] A. Gudat, S. Haag, R. Kniep, A. Rabenau *Z. Naturforsch. B* **1990**, *45*, 111 – 120.
[4] D. A. Vennos, F. J. DiSalvo, *J. Solid State Chem.* **1992**, *100*, 318; D. A. Vennos, F. J. DiSalvo, *ibid*. **1992**, *100*, 401.
[5] D. A. Vennos, M. E. Badding, F. J. DiSalvo, *Inorg. Chem.* **1990**, *29*, 4059.
[6] A. Tennstedt, C. Röhr, R. Kniep, *Z. Naturforsch. B* **1993**, *48*, 1831.
[7] D. H. Gregory, M. G. Barker, P. P. Edwards, D. J. Siddons, *Inorg. Chem.* **1995**, *34*, 5195 – 5198.
[8] Review: R. Kniep, *Pure Appl. Chem.* **1997**, *69*, 185 – 191. Some of the known nitridoferrates, -cobaltates, -nickelates, and -cuprates contain short T···T contacts (T = 3d element) within the complex anions, which were discussed as bonding interactions. In all cases, however, the T···T units are bridged by at least one nitrido group.
[9] M. Martin, B. Rees, A. Mitschler, *Acta Crystallogr. Sect. B* **1982**, *38*, 6 – 15.
[10] R. Bau, S. W. Kirtley, T. N. Sorrell, S. Winkarno, *J. Am. Chem. Soc.* **1974**, *96*, 988.
[11] Crystal structure data for $Li_6Ca_2[Mn_2N_6]$ at $T = 275$ K: trigonal, space group $R\bar{3}$ (no. 148), $a = 574.43(6)$, $c = 1856.0(2)$ pm, $V = 530.4(1)$ Å^3, $Z = 3$, $\rho_{calcd} = 2.97$ g cm^{-3}; Siemens P4 diffractometer ($Mo_{K\alpha}$ radiation, graphite monochromator); $2\theta_{max} = 60°$, 523 measured reflections, 340 symmetry-independent reflections, Lorentzian and polarization corrections, structure solution with direct methods[11a]; refinement by least squares with SHELX-97[11b]; 26 refined parameters, R values ($I \geq 2\sigma(I)$): $R1 = 0.019$, $wR2 = 0.057$; residual electron density: 0.49/ – 0.44 e$^-$ × 10^{-6} pm^{-3}. Further details of the crystal structure investigations may be obtained from the Fachinformationszentrum Karlsruhe, D-76344 Eggenstein-Leopoldshafen, Germany (fax: (+49) 7247-808-666; e-mail: crysdata@fiz-karlsruhe.de), on quoting the depository number CSD-408324. a) G. M. Sheldrick, SHELX-97, Program for the Solution of Crystal Structures, Göttingen, Germany, **1997**.; b) G. M. Sheldrick, SHELX-97, Program for the Refinement of Crystal Structures, Göttingen, Germany, **1997**.
[12] W. Klingen, R. Ott, H. Hahn, *Z. Anorg. Allg. Chem.* **1973**, *396*, 271 – 278.
[13] R. Pfeiff, R. Kniep, *J. Alloys Compd.* **1992**, *186*, 111 – 133.
[14] There are no indications for any defect occupation of the lithium positions, which would influence on the oxidation state of manganese.
[15] Interatomic distances [pm] in the crystal structure of $Li_6Ca_2[Mn_2N_6]$: Li – N 199.9(4) – 220.9(4) ($Li_7[MnN_4]$,[1] 202 – 224), Ca – N 251.7(2) – 263.5(2) ($Ca_3[MnN_3]$,[6] 239 – 275), Mn – N 177.8(2) ($Ca_3[MnN_3]$,[6] 179 and 180), Mn – Mn 235.8(1).
[16] P. Gazzara, R. M. Middleton, R. J. Weiss, *Acta Crystallogr.* **1967**, *22*, 859 – 862.
[17] The TB-LMTO program[17a] with exchange correlation potentials[17b] was used. The radial scalar relativistic Dirac equation was solved to calculate the partial waves. Empty spheres (E1 – E3) were positioned in the intermediate regions to avoid overlap of the atomic spheres within the ASA approximation (ASA with correction[17c]). The following radii [Å] for atomic and empty spheres were used: r(Li) = 1.35, r(Ca) = 1.89, r(Mn) = 1.11, r(N) = 0.92, r(E1) = 0.96, r(E2,E3) = 0.74. a) G. Krier, O. Jepsen, A. Burkhardt, O. K. Andersen, The Program TB-LMTO-ASA, Version 4.6, Max-Planck-Institut für Festkörperforschung, Stuttgart, **1995**; b) U. Barth, L. Hedin, *J. Phys. C* **1972**, *5*, 1629; c) O. K. Andersen, Z. Pawlowska, O. Jepsen, *Phys. Rev. B* **1986**, *34*, 5253.
[18] Within the density functional theory, the ELF is evaluated from the local kinetic energy density according to Pauli ($t\rho(r)$); $t\rho(r)$ is the part of the local kinetic energy density $t(r)$ due to the Pauli principle.[18a–c] At each point r, the ELF is relative to the value for a homogeneous electron gas with the density $\rho(r)$: $ELF = \{1 + [t_\rho(r)/t_{\rho,h}(\rho(r))]^2\}^{-1}$.

  1433-7851/98/3711-1584 $ 17.50+.50/0

a) A. D. Becke, K. E. Edgcombe, *J. Chem. Phys.* **1990**, *92*, 5397; b) A. Savin, A. D. Becke, J. Flad, R. Nesper, H. Preuss, H. G. von Schnering, *Angew. Chem.* **1991**, *103*, 421 – 424; *Angew. Chem. Int. Ed. Engl.* **1991**, *30*, 409 – 412; c) A. Savin, O. Jepsen, J. Flad, O. K. Andersen, H. Preuss, H. G. von Schnering, *ibid.* **1992**, *104*, 186—188; **1992**, *31*, 187 – 188.
[19] R. F. W. Bader, *Atoms in Molecules: A Quantum Theory*, Oxford University Press, Oxford, **1990**.
[20] B. Silvi, A. Savin, *Nature* **1994**, *371*, 683.
[21] A. Savin, B. Silvi, F. Colonna, *Can. J. Chem.* **1996**, *74*, 1088.
[22] A. Savin, R. Nesper, S. Wengert, T. Fässler, *Angew. Chem.* **1997**, *109*, 1892 – 1918; *Angew. Chem. Int. Ed. Engl.* **1997**, *36*, 1808 – 1832.
[23] U. Häusermann, S. Wengert, R. Nesper, *Angew. Chem.* **1994**, *106*, 2150 – 2154; *Angew. Chem. Int. Ed. Engl.* **1994**, *33*, 2069 – 2073.
[24] M. Kohout, A. Savin, *Int. J. Quantum Chem.* **1996**, *60*, 875.
[25] Diminishing influence of the d electrons on the absolute value of ELF: M. Kohout, A. Savin, *J. Comput. Chem.* **1998**, in press.

An Efficient Venus Flytrap for the Reversible Binding of Nitric Oxide**

Rajendra Rathore, Sergey V. Lindeman, and Jay K. Kochi*

Intermolecular noncovalent binding of guest molecules by synthetic macromolecular hosts has been a rapidly growing field of research[1] since the first discovery of crown ethers by Pedersen.[2] The unique chemical and physical properties of these novel host – guest structures are the key to the future development of nanomolecular devices, chemosensors, etc.[3] Here we describe the synthesis of a novel *cis*-stilbenoid hydrocarbon ligand which strongly binds a neutral diatomic molecule such as nitric oxide (NO), which is of significant biological interest.[4]

The hydrocarbon ligand 1,2-bis(pentamethylphenyl)bicyclo[2.2.2]oct-2-ene (Venus flytrap, VFT)[5] possesses a unique molecular structure in which a pair of pentamethylphenyl moieties are forced to be closely juxtaposed in a cofacial manner by the very rigid bicyclooctene framework, as established by X-ray crystallography.[6]

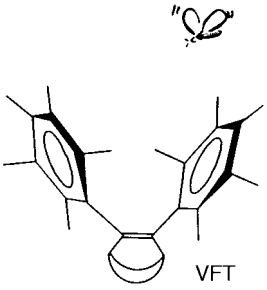

The activation of VFT by oxidation in dichloromethane readily generates the persistent cation radical $VFT^{+\bullet}$,[7] which upon exposure to gaseous nitric oxide leads immediately to a bright blue solution. Quantitative IR spectroscopic analysis of the blue solution indicates the complete uptake of nitric oxide, as judged by observing the characteristic absorption at 1885 cm^{-1} for a single N–O stretching frequency.[8] The high stability of blue $[VFT \cdot NO]^+$ allows the ready isolation of a single crystal from a mixture of dichloromethane and toluene at $-23\,^{\circ}C$. X-ray crystallography established its molecular structure to be made up of a single molecule of nitric oxide trapped between two cofacial phenyl rings. The diatomic nitric oxide fits neatly within the cavity of VFT, where it lies parallel to one of the phenyl rings, as shown by the space-filling representation in Figure 1.

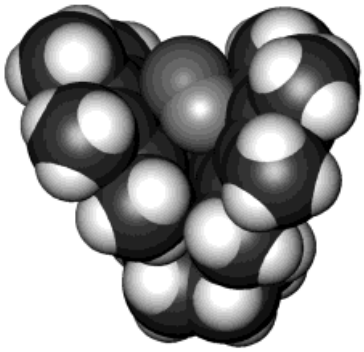

Figure 1. Space-filling representation of NO tightly entrapped within the VFT cleft.

The N–O bond distance of 1.12 Å in $[VFT \cdot NO]^+$ is consistent with a noncovalently bonded nitric oxide molecule,[9] especially since the separation between the nitrogen atom and any aromatic carbon atom (av 2.5 Å) is much greater than the covalent N–C bonding distance.[10] Moreover, most of the positive charge resides on the aromatic and olefinic carbon atoms, as judged by the significant lengthening of the average C_{arene}–C_{arene} distance (1.42 Å) with respect to that in the neutral stilbenoid ligand.[11] Thus, VFT acts as a molecular tweezer for neutral NO. This is readily apparent upon inspection of the phenyl rings, which are significantly arched in an attempt to encapsulate the NO molecule. The distortion of the pentamethylphenyl groups is shown in Figure 2.[12]

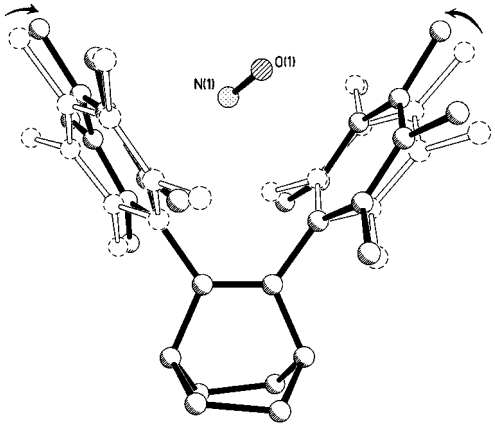

Figure 2. The superimposed molecular structures of the neutral stilbenoid ligand VFT (dashed line) and $[VFT \cdot NO]^+$ (solid line); hydrogen atoms have been omitted for clarity.[12]

[*] Prof. J. K. Kochi
Department of Chemistry
University of Houston
Texas 77204-5641 (USA)
Fax: (+1) 713-743-2709
E-mail: cjulian@pop.uh.edu

[**] We thank the National Science Foundation and the Robert A. Welch Foundation for financial support.

  1433-7851/98/3711-1585 $ 17.50+.50/0